Corrosion Best Practice: Creating Pipe-flow Conditions Using a Rotating Cylinder Electrode

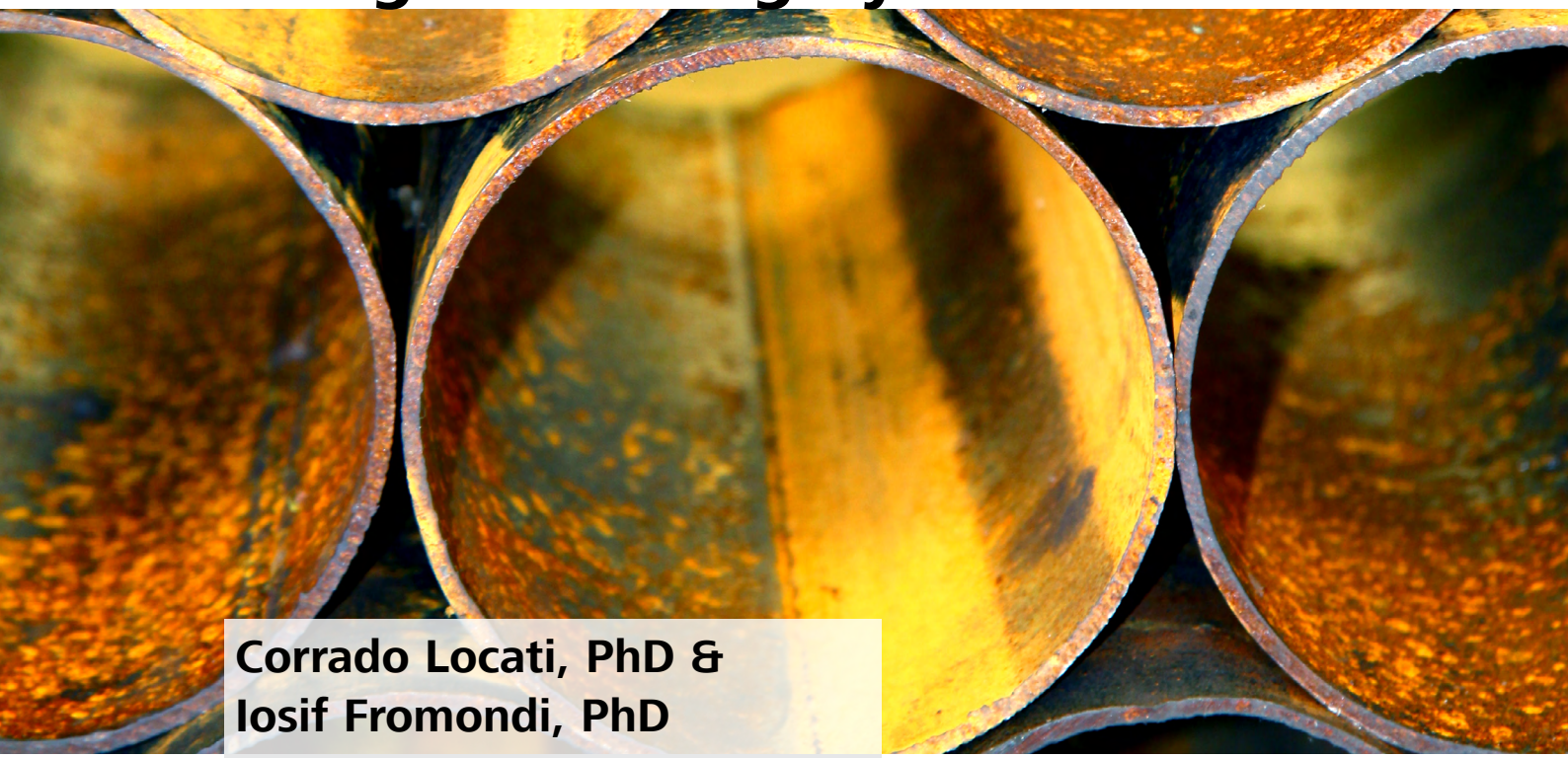

Corrado Locati, PhD &
Iosif Fromondi, PhD

Electrochemical measurements utilizing a rotating cylinder electrode (RCE) are widely used in industrial corrosion applications when simulation of realistic pipe conditions are necessary in a lab environment. RCE measurements, along with rotating disk electrode (RDE) and rotating ring-disk electrode (RRDE) measurements, fall under the group of hydrodynamic electrochemical experiments which are characterized by forced convection conditions.

This white paper allows further insight into the particularities and parameters which govern the electrochemical measurements, in particular measurements performed in turbulent flow conditions (i.e., using a rotating cylinder electrode), and shows a complete picture of the best practice use of this technique. The annexes provide an overview and short explanation of the parameters and laws specific to the fluid behavior in electrochemical cells with RCE.

Metrohm
Autolab

02 Introduction

General aspects of mass transport in electrochemistry

To have a good understanding and clearly differentiate between electrochemical experiments conducted in static or hydrodynamic conditions, a general overview of the theoretical aspects of mass transport and flux is presented.

Current vs flux of material through the electrolyte

For an electrochemical reaction (i.e. exchange of electrons) to take place at the surface of an electrode, the electrochemically active species need to reach the surface of the working electrode.

The total mass transport of material, from the electrolyte to the working electrode, is completely characterized by the Nernst-Planck equation:

$$J_{(x,t)} = -D\left(\frac{\partial C_{(x,t)}}{\partial x}\right) - \frac{zF}{RT} D C_{(x,t)}\left(\frac{\partial \phi_{(x,t)}}{\partial x}\right) + C_{(x,t)} \nu_{(x,t)} \quad (1)$$

All the contributions are functions of distance «x» from the electrode surface.

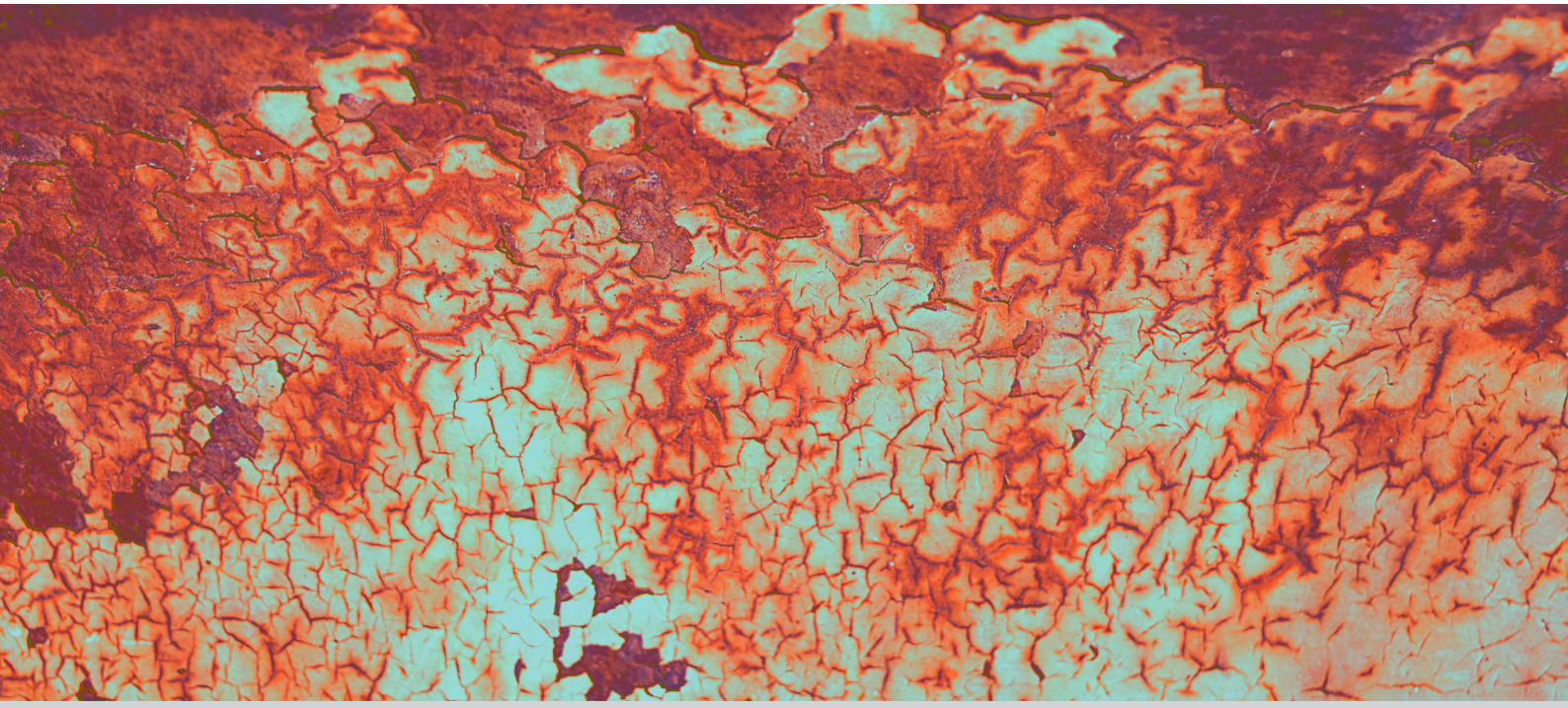

The Nernst-Planck equation shows that the flux of material towards the electrode surface is proportional to the diffusion, through the gradient of the concentration $-D\left(\frac{\partial C_{(x,t)}}{\partial x}\right)$, to migration, through the gradient of the electrostatic potential $-\frac{zF}{RT} D C_{(x,t)}\left(\frac{\partial \phi_{(x,t)}}{\partial x}\right)$, and to convection, through stirring the solution $C_{(x,t)} \nu_{(x,t)}$, which results in a hydrodynamic velocity.

The current measured at the working electrode depends directly on the flux of species from the bulk electrolyte to the working electrode, and can be calculated by using the following equation:

$$i_t = nFAJ_{(x,t)} \quad (2)$$

Measurements under diffusion control

It is possible to set up an experiment in such a way that the migration and convection terms can be neglected. The migration term can be eliminated by adding a supporting electrolyte 10–100 times in excess compared to the redox couple of interest. In this way, the electric field between the working and counter electrodes (the two electrodes involved in the redox reaction) is dissipated over all ions in solution and not just over the electroactive material. The convection contribution can be eliminated by keeping the solution unstirred. When both the migration and the convection contributions are neglected, the limiting factor in the flux of species at the electrode is only the mass transport due to diffusion.

Measurements under convection conditions

In the case of experiments conducted with rotating working electrodes, such as rotating disk electrodes (RDEs), rotating ring-disk electrodes (RRDEs) and rotating cylinder electrodes (RCEs), the rotation of the electrode in the electrolyte generates a stirring of the solution. Therefore the hydrodynamic segment of the Nernst-Planck equation cannot be neglected anymore. Experiments with rotating electrodes, also known as **hydrodynamic measurements**, have the benefit of providing mass transport of electroactive species in solution by **diffusion and convection**, instead of diffusion alone. The convection leads to enhanced mass transport conditions, which in turn facilitates the reduction of its influence on the overall measured current. This allows for a complete characterization of electrode kinetics.

Hydrodynamic measurements: Laminar and turbulent flow

During hydrodynamic experiments using RDEs and RRDEs, a well-defined **laminar** flow is formed at the surface of the rotating electrodes, even at higher rotation rates.

Schematic drawings of RDE (A), RRDE (B) and RCE (C) electrodes are shown in **Figure 1**. The difference between these types of electrodes lies in the position of the active material surface (usually a metal or glassy carbon, shown in grey) with respect to the PEEK body (shown in beige).

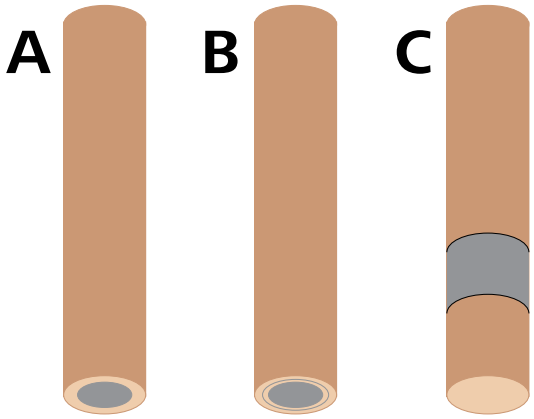

Figure 1.

A: Rotating disk electrode (RDE)
B: Rotating ring-disk electrode (RRDE)
C: Rotating cylinder electrode (RCE)

LAMINAR FLOW: fluid travels smoothly, in a regular way with each layer of the fluid passing by the adjacent layers with little or no mixing. The velocity, pressure, and other flow properties at each point in the fluid for a given flow rate will be constant and well known.

TURBULENT FLOW: fluid undergoes irregular fluctuations that mix along the flow path between the layers, and the flow parameters and flow properties are not constant.

In the case of the RDE and RRDE, the kinetic parameters can be determined from the limiting current, by using the well-known **Levich** equation (for RDE, **Equation 3**):

$$i_L = 0.620\, nFA\, D^{2/3} \omega^{1/2} \nu^{-1/6} C \quad (3)$$

and **Koutecký-Levich** equation (**Equation 4**):

$$\frac{1}{i} = \frac{1}{i_k} + \frac{1}{i_{mt}} \quad (4)$$

A classic application example based on the use of rotating electrodes is the oxygen reduction reaction (ORR), which has been extensively studied by using RDEs and RRDEs.

Rotating Cylinder Electrodes (RCE)

Rotating cylinder electrodes (RCE) are different from the rotating disk and ring-disk electrodes (RDE and RRDE) by the position of the electrode material in the housing. While for the RDE and RRDE the surface of the electroactive material is perpendicular to the direction of the convective-diffusive mass transport, in the case of the RCE, the surface of the electrode material is radially aligned with the convective-diffusive mass transport direction (**Figure 2**). This leads to a difference in the convective regime which is generated during the rotation at the surface of the electrode material.

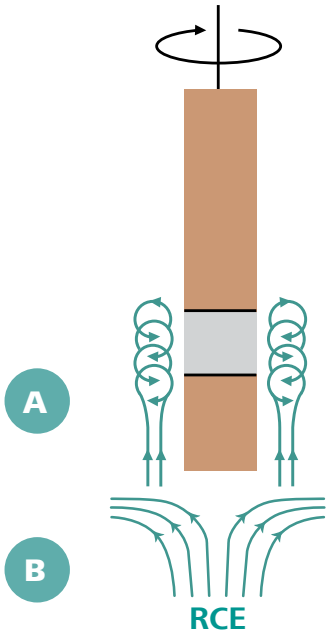

Figure 2.

A **Turbulent Flow** **B** **Laminar Flow**

The Rotating Cylinder Electrode is exposed to a turbulent flow. The Rotating Disk and Rotating Ring Disk Electrode are exposed to laminar flow.

As a consequence, the convective flow generated by the RCEs is **turbulent** even in in solutions with low kinematic viscosity (i.e. low Reynolds numbers) as opposed to the RDE and RRDE electrodes where the generated flow is laminar, even in solutions with high kinematic viscosity (i.e. high Reynolds numbers).

Real-world flow conditions are mainly turbulent. Therefore, the ability to create and quantify turbulent flow conditions on a laboratory scale makes it possible to simulate realistic situations in the laboratory. Perhaps the most commonly encountered practical use of the RCE is creating the mass transport conditions which occur in pipes (where enhanced mass transport directly influences the corrosion rate of the pipe material) in the laboratory environment.

As opposed to the hydrodynamic electrochemical measurements performed in laminar flow conditions (i.e. typical RDE and RRDE experiments), where the equation describing the mass transport at the surface of the electrode has an analytical solution, when performing measurements in turbulent flow conditions, the convective-diffusive mass transport equations cannot be solved analytically but only with numerical solutions. Additionally, the numerical solution is directly dependent on the size, dimension, construction and roughness of the RCE.

Rotating Cylinder Electrode - typical applications

Depending on the scope of the experiment, RCEs are used together with most of the major electrochemical techniques. The RCE is used with chronopotentiometry (measuring the electrode potential in time) and chronoamperometry (measuring the current in time) techniques to retrieve information about the existence and stability of surface films and to monitor the mass transport as function of the rotation speed, respectively.

The most common potential sweep techniques are used together with an RCE for electrochemical corrosion and the investigation into other electrode surface properties.

RCE in industrial corrosion

Corrosion rate analysis and the study of the corrosion rate as a function of the rotation rate (i.e convective flux) is one of the most common applications for the RCE. Corrosion studies are also done by using electrochemical impedance spectroscopy (EIS) and electrochemical noise (ECN), showing the same corrosion current dependence on the rotation rate.

As noted earlier, RCE is often used for corrosion analysis of pipe materials by simulating the flow conditions occurring in pipelines in a laboratory environment. One common use of the RCE is in oil and gas industry where the effect of different corrosion inhibitors on the pipe materials is investigated by using linear polarization (LP) or electrochemical impedance spectroscopy (EIS) techniques.

Also, the behavior of the protective coatings can be investigated with the RCE simply in the laboratory, avoiding the need for direct and expensive measurements on site at the pipelines themselves.

Below are some other examples of situations where the RCE measurements are used:

- cathodic protection studies
- tribocorrosion
- nanofluidic studies
- metal recovery
- metal release measurements in water monitoring
- decontamination systems

06 Rotating Cylinder Electrode: Typical parameters and terminology

Limiting current in RCE

A Levitch-like expression for the RCE can be derived by using and combining individual equations (see ANNEX 1):

$$i_{L\,(RCE)} = nFACK_m \qquad (5)$$

From **Equation 5** and the dependence on K_m, it can be concluded that the current $i_{L(RCE)}$ changes with the linear velocity of the RCE, raised to the power of 0.7 ($v_{RCE}^{0.7}$). This can be easily verified experimentally with the logarithm of the current, log(i), plotted against the logarithm of the linear velocity, log(v_{RCE}). If a slope of 0.7 is observed, the measured current is consistent with the Levich-like equation.

Relationship between RCE rotation rate and fluid velocity in the pipe

In a typical RCE experiment, the liquid used as electrolyte is identical to the liquid present in the pipe material under investigation. The RCE cylindrical insert is composed of the same material as the pipe. In order to model the turbulent flow in a pipe of defined dimensions and material, a rotation rate F_{rot} is applied to the RCE. This rate is related to the velocity of the fluid in the pipe (**Equation 6**):

$$F_{RCE} = \left(K_s d_{RCE}^{\frac{3}{4}}\, d_p^{-\frac{5}{28}} \nu^{-0.25} S_C^{-0.086} \nu_p^{1.250}\right)\left(\frac{60}{2\pi}\,\frac{1}{r_{RCE}}\right) \qquad (6)$$

For example, it is possible to simulate a flow of 100 cm s^{-1} in a pipe with a Schedule of 40 (see next column) and an internal diameter of 10.23 cm (4 inches) by rotating the RCE at 680 RPM. The reverse can also be done: by rotating a RCE at 1200 RPM, a flow of 142.7 cm s^{-1} can be simulated in a pipe with an internal diameter of 5 cm.

Terminology: Pipe schedule number, SCH

Pipes are usually characterized by an external diameter d_p (cm) and a **schedule number** *SCH*, which is a dimensionless quantity related to the pipe wall thickness. The schedule number is a measure of the maximum internal pressure the pipe can withstand with the allowable tensile stress of the material.

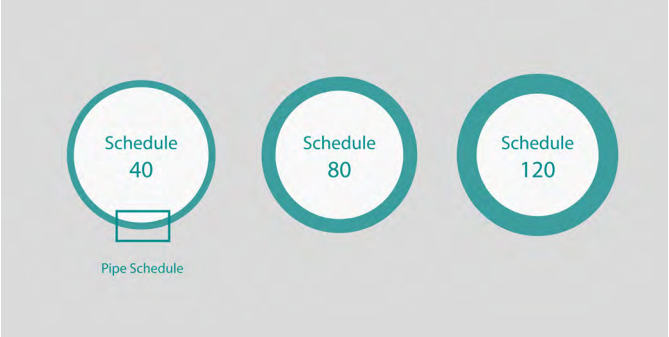

Figure 3.

Exemplification of pipe schedule.

The pipe dimensions are related to the schedule number (*SCH*) according to the following equation:

$$SCH = 1000\,\frac{P}{S} \qquad (7)$$

Rotating Cylinder Electrode - measurement example

As a measurement example, the influence of a corrosion inhibitor on the rate of corrosion measured in turbulent flow conditions (RCE) is presented. Linear polarization (LP) experiments were performed using a RCE with a carbon steel cylindrical insert.

The influence of the rotation rate (i.e. convection) on the corrosion parameters is discussed in the dedicated Metrohm Autolab application note (**AN-COR-015**).

Experimental conditions and results

Two LP experiments were conducted: one without using a corrosion inhibitor, and one with a corrosion inhibitor present in the electrolyte. The material of the RCE cylindrical insert (working electrode) was carbon steel (1018) (density ρ = 7.87 g cm^{-3}; equivalent weight *EW* = 27.93). The electrochemical cell was completed with an Ag/AgCl, 3 M KCl reference electrode and two stainless steel rods as counter electrodes.

The electrolyte was composed of an aqueous solution containing 0.5 mol/L HCl and 0.5 mol/L NaCl. For testing the influence of the inhibitor on the corrosion rate, 4 mL of corrosion inhibitor (tryptamine, 1000 mg/L, 0.78 mol/L) in ethanol was added to the same electrolyte.

The RCE electrode was rotated at 500 RPM, corresponding to a fluid velocity v_{RCE} = 82.3 cm s^{-1} (2.7 ft s^{-1}) inside of a schedule 40 pipe, with an internal diameter of 30.32 cm (12 inches).

After monitoring the open circuit potential (OCP) for five minutes, LP measurements were conducted from –20 mV to +20 mV vs. OCP, with a scan rate of 1 mV s^{-1}, at ambient room temperature.

All data was measured and analyzed with the NOVA software. The i vs E plots resulting from the LP measurements are shown in **Figure 4**. The data measured without the corrosion inhibitor is displayed in blue, and the data corresponding to the results obtained with the corrosion inhibitor being used is presented in red.

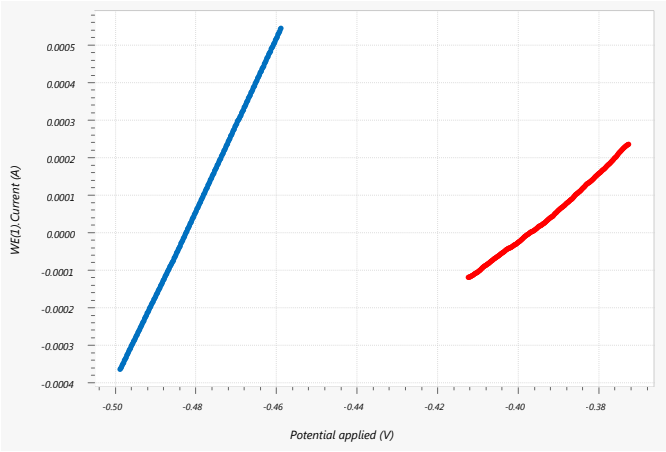

Figure 4.

i vs E plot from LP measurement without inhibitor in blue, with inhibitor in red.

A visual inspection of **Figure 4** shows that the *i vs E* plot which contains the corrosion inhibitor lies to the right of the corresponding plot measured without any inhibitor in the electrolyte. Consequently, the results show a corrosion potential $E_{corr,i}$ = –0.392 *V* vs. Ag/AgCl in the case of the solution with the inhibitor, and E_{corr} = –0.479V vs. Ag/AgCl in the case of the solution without inhibitor added.

Applying a linear regression around the OCP, the polarization resistance (R_p) was calculated (as the inverse of the slope of the regression line), resulting a higher polarization resistance R_p when the inhibitor is present. The calculated R_p without inhibitor is R_p = 42.62 Ω, and with the corrosion inhibitor $R_{p,i}$ = 135.96 Ω.

The Tafel analysis is also performed as part of the corrosion rate analysis tool in NOVA (**Figure 5**).

The summary of the corrosion rate analysis calculated from the linear regression and the Tafel analysis, both with and without the corrosion inhibitor, is presented in **Table 1**. The calculated values of the corrosion rates (in *mm/year*) are also listed. The corrosion rate for the solution with the inhibitor (0.065 *mm/year*) is substantially lower than the corrosion rate without inhibitor (0.25 *mm/year*).

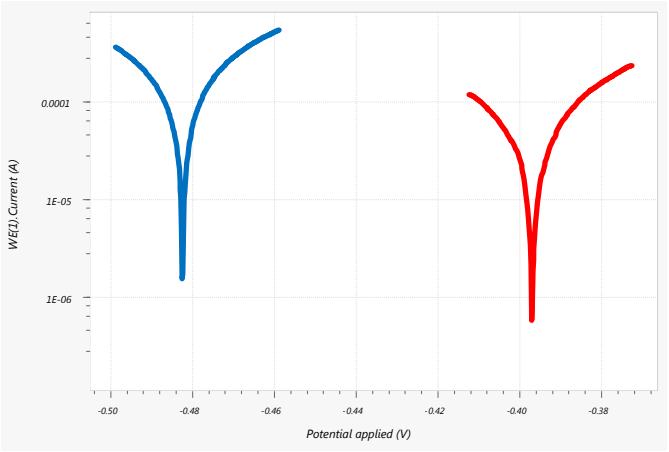

Figure 5.
Tafel plots of the data taken without corrosion inhibitor in blue, and with inhibitor in red.

Table 1. Data presented from linear regression and Tafel analysis from the experiments with and without addition of the corrosion inhibitor.

Corrosion parameter	No Inhibitor	With Inhibitor
E_{corr} (*V*) from linear regression	-0.479	-0.392
E_{corr} (*V*) from Tafel analysis	-0.482	-0.396
R_p (Ω) from linear regression	42.62	135.96
R_P (Ω) from Tafel analysis	43.32	136.39
Corrosion rate (*mm/year*) from Tafel analysis	0.25	0.065

ASTM Standard using Rotating Cylinder Electrode

The ASTM Standard G185 defines the practice for evaluating corrosion inhibitors using the RCE. The linear polarization resistance (LPR) and electrochemical impedance spectroscopy (EIS) measurements are listed as possible electrochemical techniques which can be used, as well as mass loss determination and pitting corrosion evaluation.

According to this ASTM standard, the inhibitor efficiency can be calculated with the following equation:

$$\text{Inhibitor efficiency}\ (\%) = 100 \cdot \frac{CR_{no\ inhib} - CR_{inhib}}{CR_{no\ inhib}} \quad \textbf{(8)}$$

The parameter $CR_{no\ inhib}$ (*mm/year*) is the corrosion rate without inhibitor, and CR_{inhib} (*mm/year*) is the corrosion rate calculated in the presence of the inhibitor.

For the example used in this publication (pages 7–8), the inhibitor efficiency is calculated at 74%.

Acceptable inhibitor efficiency varies between industries. Check first with your quality officer to determine the appropriate parameters for your business.

Conclusion

Electrochemical corrosion measurements bring a deeper understanding of corrosion phenomena, allowing an investigation of corrosion mechanisms as well as the influence of external parameters on the rate of corrosion. Results obtained by using electrochemical methods are more accurate, and the measurements are much faster when compared with the classical corrosion investigation methods (e.g., salt spray chamber methods), leading to both improved efficiency and productivity of any corrosion measurement laboratory.

One of the parameters which influences the corrosion process in a certain environment is the flow of the liquid close to the surface of the corroding material (also see application note **AN-COR-015**). As briefly covered in this white paper, electrochemical measurements using RCEs successfully simulate real-life pipe flow systems (i.e. liquid flowing through a pipe) in a laboratory environment, allowing efficient and accurate quantification of the corrosion process occurring in these types of systems.

The existing ASTM G185 standard further supports the robustness of the RCE methods for industrial corrosion applications by utilizing them while evaluating and qualifying oil field and refinery corrosion inhibitors.

References

- Maciel J.M.; Agostinho S.M.L. Construction and characterization of a rotating cylinder electrode for different technological applications, *J. Appl. Electrochem*. 1999, *29*, 741–745
- Soliman, H.M.A.; Abdel-Rahman, H.H. The use of rotating cylinder electrode to study the effect of 1,3-dihydroxypropane on copper electrorefining, Port. *Electrochim. Acta,* 2006, *24*, 415–440
- Gabe D.R.; Wilcox G.D.; Gonzalez-Garcia J.; Walsh F.C. The rotating cylinder electrode: its continued development and application, *J. Appl. Electrochem.* 1998, *28*, 759–780
- The rotating cylinder electrode for studies of corrosion engineering and protection of metals – an illustrated review, A revised review for Corrosion Science, F.C. Walsh et al, 21 March, 2017
- Standard practice for evaluating and qualifying oil field and refinery corrosion inhibitors using the rotating cylinder electrode, ASTM G185-06

Metrohm Application Notes

We created a number of application notes that can help your battery research and development:

- Calculation of Corrosion Parameters with NOVA
- Measurement of Polarization Resistance
- Corrosion Inhibitors
- Corrosion Rates Measurements in Quiescent and Turbulent Flow Condition

To find these free application notes, visit the Metrohm Application Finder (**metrohm.com/applications**). The list above is subject to change and you can use a Full Text Search «**AN-COR**» to discover additional battery applications as they become available.

Dedicated to research

www.metrohm.com/electrochemistry

Metrohm Autolab

WP-055EN by Metrohm, published 02-2020

ANNEX 1 – Useful parameters and formulas used in RCE fluidics

To further understand how an RCE experiment can model the corrosion in a pipeline, it is helpful to understand the parameters and properties of fluids, the characterization of different mass transport phenomena, and also the terminology used for the characterization of pipes.

Reynolds number, R_e

The fluid flow is characterized by the dimensionless **Reynolds number**, R_e, defined as the ratio between the velocity u of the fluid and the kinematic viscosity ν:

$$R_e = uL\frac{\rho}{\mu} = \frac{uL}{\nu} \qquad \textbf{A1}$$

The Reynolds number is used to predict the transition from laminar to turbulent flow. At low Reynolds numbers, flows are dominantly laminar with sheet-like movement. At high Reynolds numbers, turbulence results from differences in the speed and direction of the fluid movement.

For a rotating cylinder electrode, the Reynolds number is given by:

$$R_e = v_{RCE}\, d_{RCE}\frac{\rho}{\mu} \qquad \textbf{A2}$$

For an RCE, turbulent flow is typically achieved when $R_e > 200$.

Linear velocity, v_{RCE}

The **linear velocity** v_{RCE} (cm s^{-1}) is given by:

$$v_{RCE} = \frac{\omega}{2} d_{RCE} = \frac{\pi}{60} F_{rot}\, d_{RCE} \qquad \textbf{A3}$$

As can be seen from Equations A2 and A3, both the cylinder diameter and the rotation rate have a direct influence on the the Reynolds number. Therefore, a turbulent flow can be achieved by using either a larger cylinder diameter, a higher rotation rate, or both in combination.

Mass Transport Characterization

Viscosity

The transport of momentum inside of a fluid is characterized by the viscosity, which is the measure of how a fluid resists deformation. A fluid can be modeled as if composed of different layers, each moving with a velocity relative to the other layers. The frictional force between these layers is proportional to the viscosity of the fluid.

Convective mass transfer

The convective mass transfer is the transport of material between a boundary surface, such as the electrode surface, and a moving fluid.

There are two kinds of convection:

- Forced convection: the fluid moves due to an external force, e.g. the stirring of an electrode which causes a difference of pressure in the electrolyte
- Natural convection: the fluid moves under the variation of density, due to temperature and concentration differences

Kinematic viscosity, ν

The momentum diffusivity, also known as kinematic viscosity, is defined as the ratio between the viscosity of the fluid and its density:

$$\nu = \frac{\mu}{\rho} \qquad \text{A4}$$

Thermal diffusivity, α

The thermal diffusivity measures the rate transfer of heat from hot to cold areas in the fluid.

$$\alpha = \frac{k}{\rho c_p} \qquad \text{A5}$$

In the case of the rotating cylinder electrode, the thermal diffusivity term is generally not used.

Mass diffusivity, J

The mass diffusivity, diffusion, or diffusion coefficient, relates the molar flux (due to molecular diffusion) and the gradient in the concentration of the species:

$$J = -D\left(\frac{\partial C}{\partial x}\right) \qquad \text{A6}$$

Dimensionless parameters (such as the ratio of the two out of the three above-mentioned quantities) are often used to correlate convective transfer data.

Schmidt number, S_C

The Schmidt number, S_C, defines the ratio between the momentum diffusivity (the kinematic viscosity) and the diffusive mass transfer. It describes the transport properties of the electrolyte, and it is given by the following equation:

$$S_C = \frac{\nu}{D} = \frac{\mu}{\rho D} \qquad \text{A7}$$

When $S_C > 1$, the diffusion of species at the electrode-electrolyte interface is due predominantly to the stirring of the solution. When $S_C < 1$, the diffusion is due predominantly to natural convection.

Sherwood number, S_H,

The Sherwood number, S_H, is the ratio between the convective mass transfer $K_m d_{RCE}$ and the diffusive mass transfer D. It describes the mass transport due to forced convection, and it is given by:

$$S_H = \frac{K_m d_{RCE}}{D} = 0.0791\, R_e^{0.7} S_C^{0.356} \qquad \text{A8}$$

Convective mass transfer coefficient K_m

The convective mass transfer coefficient K_m (cm s^{-1}) measures the rate of the mass transfer between the bulk electrolyte and the electrode-electrolyte interface, under convection.

$$K_m = S_H \frac{D}{d_{RCE}} = \left(0.0791\, R_e^{0.7} S_C^{0.356}\right)\frac{D}{d_{RCE}} \qquad \text{A9}$$

The convective mass transfer coefficient can be expressed as function of the linear velocity of the fluid U_{RCE}, in cm s^{-1}, (Equation A10), as function of the rotation rate of the RCE in *Hz*, ω_{RDE}, (Equation A11), or as function of the rotation rate of the RCE in RPM, F_{RCE}, (Equation A12):

$$K_m = 0.0791\, d_{RCE}^{-0.3}\, \nu^{-0.344}\, D^{0.644}\, \nu_{RCE}^{0.7} \qquad \text{A10}$$

$$= 0.0487\, d_{RCE}^{0.4}\, \nu^{-0.344}\, D^{0.644}\, \omega_{RCE}^{0.7} \qquad \text{A11}$$

$$= 0.0051\, d_{RCE}^{0.43}\, \nu^{-0.344}\, D^{0.644}\, F_{RCE}^{0.7} \qquad \text{A12}$$

Wall shear stress, τ_{RCE}

Finally, turbulent flow at the surface of the RCE induces a **wall shear stress** τ_{RCE} (g cm^{-1} s^{-2}), parallel to the RCE surface. This is quantified by:

$$\tau_{cyl} = 0.0791\, \frac{\rho\, R_e^{-0.3}\, r_{cyl}^2\, F_{rot}^2}{10} \qquad \text{A13}$$

ANNEX 2 - Physical and chemical constants used in the calculation examples provided in the present White Paper.

Table 1: Physical and chemical constants used in the calculation examples provided in the present White Paper.

Name	Value	Unit	Symbol	Notes
Concentration	1.00E-06	mol cm^{-3}	C	Bulk concentration, assume 1 x 10^{-6} for pure water
Density	0.997	g cm^{-3}	ρ	Density of the solution, 0.99713 for pure water at STP
Absolute Viscosity	0.00894	g cm^{-1} s^{-1}	μ	Also called dynamic viscosity, assume 0.00891 for pure water at STP
Kinematic Viscosity	0.00896	cm^2 s^{-1}	ν_k	Absolute viscosity divided by density, assume 0.00894 for pure water at STP
Diffusion Coefficient	1.00E-05	cm^2 s^{-1}	D	For the bulk species, assume 1 x 10^{-5} for pure water at STP
Number of Electrons	1	–	z	Number of electrons transferred per reaction, if in the bulk
RCE diameter	12	mm	d_{RCE}	Diameter of RCE cylinder insert
RCE cylinder Insert Diameter	1.20	cm	d_{rce}	Diameter of RCE cylinder insert
RCE cylinder Insert Radius	0.60	cm	r_{rce}	Radius of RCE cylinder insert
RCE cylinder Insert Height	0.80	cm	h_{rce}	Height of RCE cylinder insert
RCE cylinder Insert Area	2.997	cm^2	A_{rce}	Exposed area of RCE cylinder insert
Critical Reynolds Number	200	-	RE_{crit}	The minimum Reynolds number to ensure turbulent flow
Critical Rotation Rate	2.49	rad s^{-1}	ω_{crit}	The critical rotation rate to achieve RE = 200 with the 12 mm diameter RCE
Critical Rotation Rate	24.00	RPM	F_{crit}	The critical rotation rate to achieve RE = 200 with the 12 mm diameter RCE
Minimum Rotation Rate	100	RPM	$\upsilon_{max,RPM}$	Minimum rotation rate allowed by the Autolab motor controller
Maximum Rotation Rate	5000	RPM	$\upsilon_{min,RPM}$	Maximum rotation rate allowed by the RCE
Silverman Constant	0.1185	–	K_s	Constant used in calculating equivalent rotation rate
Schmidt Number	896.14	–	S_c	Kinematic viscosity divided by product of diffusion constant and density
Faraday Constant	96485	C mol^{-1}	F	Factor to convert between current and mass, C = Coulomb
Temperature	25	°C	T	
Absolute Temperature	298	K	T	

ANNEX 3 – Calculated quantities for the Autolab RCE

In **Table 2** below, the quantities calculated with the Autolab RCE at different rotation rates are shown. For rotation rates from 100 RPM to 5000 RPM, the RCE surface velocity, the Reynolds number, the Wall shear stress, the mass transfer coefficient and the limiting current and current density are listed.

Table 2 – Calculated quantities for the Autolab RCE (12 mm diameter cylinder)

Rotation Rate ω	**Rotation Rate ω**	**RCE Surface Velocity U_{cyl}**	**Reynolds Number R_e**	**Wall Shear Stress τ_{cyl}**	**Wall Shear Stress τ_{cyl}**	**Mass Transfer Coefficient K_m**	**Limiting Current i_L (RCE)**	**Limiting Current Density j_L (RCE)**
RPM	rad s^{-1}	cm s^{-1}		g cm^{-1} s^2	kg m^{-1} s^2	cm s^{-1}	A	A cm^{-2}
100	10.47197551	6.283185307	841.36991	0.41284964	0.041284964	0.000827049	0.00023916	7.980E-05
200	20.94395102	12.56637061	1682.7398	1.341352	0.1341352	0.001343545	0.00038852	0.00013
300	31.41592654	18.84955592	2524.1097	2.672379	0.2672379	0.001784499	0.00051603	0.000172
400	41.88790205	25.13274123	3365.4796	4.358067	0.4358067	0.002182596	0.00063115	0.000211
500	52.35987756	31.41592654	4206.8495	6.368555	0.6368555	0.002551587	0.00073785	0.000246
600	62.83185307	37.69911184	5048.2195	8.682585	0.8682585	0.002898926	0.00083829	0.00028
700	73.30382858	43.98229715	5889.5894	11.28388	1.1283883	0.003229237	0.00093381	0.000312
800	83.7758041	50.26548246	6730.9593	14.1594	1.4159401	0.003545637	0.0010253	0.000342
900	94.24777961	56.54866776	7572.3292	17.29833	1.729833	0.003850358	0.00111342	0.000372
1000	104.7197551	62.83185307	8413.6991	20.6915	2.0691497	0.004145065	0.00119864	0.0004
1100	115.1917306	69.11503838	9255.069	24.33097	2.4330973	0.004431045	0.00128134	0.000428
1200	125.6637061	75.39822369	10096.439	28.2098	2.8209801	0.00470932	0.00136181	0.000454
1300	136.1356817	81.68140899	10937.809	32.32181	3.2321805	0.004980715	0.00144029	0.000481
1400	146.6076572	87.9645943	11779.179	36.66144	3.6661444	0.005245911	0.00151698	0.000506
1500	157.0796327	94.24777961	12620.549	41.22371	4.1223708	0.00550548	0.00159204	0.000531
1600	167.5516082	100.5309649	13461.919	46.00403	4.600403	0.005759905	0.00166561	0.000556
1700	178.0235837	106.8141502	14303.288	50.99823	5.0998227	0.0060096	0.00173782	0.00058
1800	188.4955592	113.0973355	15144.658	56.20244	5.620244	0.006254924	0.00180876	0.000604
1900	198.9675347	119.3805208	15986.028	61.6131	6.1613096	0.006496192	0.00187852	0.000627
2000	209.4395102	125.6637061	16827.398	67.22687	6.7226872	0.006733677	0.0019472	0.00065
2100	219.9114858	131.9468915	17668.768	73.04066	7.3040664	0.006967626	0.00201485	0.000672
2200	230.3834613	138.2300768	18510.138	79.05156	7.9051564	0.007198254	0.00208154	0.000695
2300	240.8554368	144.5132621	19351.508	85.25684	8.525684	0.007425758	0.00214733	0.000716
2400	251.3274123	150.7964474	20192.878	91.65392	9.1653915	0.007650313	0.00221227	0.000738
2500	261.7993878	157.0796327	21034.248	98.24036	9.8240355	0.007872077	0.00227639	0.00076
2600	272.2713633	163.362818	21875.618	105.0139	10.501386	0.008091195	0.00233976	0.000781

Rotation Rate ω	Rotation Rate ω	RCE Surface Velocity U_{cyl}	Reynolds Number R_e	Wall Shear Stress τ_{cyl}	Wall Shear Stress τ_{cyl}	Mass Transfer Coefficient K_m	Limiting Current i_L (RCE)	Limiting Current Density j_L (RCE)
RPM	rad s^{-1}	cm s^{-1}		g cm^{-1} s^2	kg m^{-1} s^2	cm s^{-1}	A	A cm^{-2}
2700	282.7433388	169.6460033	22716.988	111.9722	11.197223	0.008307798	0.00240239	0.000802
2800	293.2153143	175.9291886	23558.357	119.1134	11.911338	0.008522008	0.00246434	0.000822
2900	303.6872898	182.2123739	24399.727	126.4353	12.643535	0.008733934	0.00252562	0.000843
3000	314.1592654	188.4955592	25241.097	133.9362	13.393622	0.008943679	0.00258627	0.000863
3100	324.6312409	194.7787445	26082.467	141.6142	14.16142	0.009151336	0.00264632	0.000883
3200	335.1032164	201.0619298	26923.837	149.4675	14.946754	0.009356993	0.00270579	0.000903
3300	345.5751919	207.3451151	27765.207	157.4946	15.749458	0.00956073	0.00276471	0.000922
3400	356.0471674	213.6283004	28606.577	165.6937	16.569373	0.009762624	0.00282309	0.000942
3500	366.5191429	219.9114858	29447.947	174.0634	17.406345	0.009962743	0.00288096	0.000961
3600	376.9911184	226.1946711	30289.317	182.6023	18.260227	0.010161155	0.00293833	0.00098
3700	387.4630939	232.4778564	31130.687	191.3088	19.130875	0.010357919	0.00299523	0.000999
3800	397.9350695	238.7610417	31972.057	200.1815	20.018154	0.010553095	0.00305167	0.001018
3900	408.407045	245.044227	32813.426	209.2193	20.92193	0.010746735	0.00310767	0.001037
4000	418.8790205	251.3274123	33654.796	218.4208	21.842075	0.010938891	0.00316323	0.001055
4100	429.350996	257.6105976	34496.166	227.7847	22.778466	0.011129612	0.00321839	0.001074
4200	439.8229715	263.8937829	35337.536	237.3098	23.730982	0.011318942	0.00327313	0.001092
4300	450.294947	270.1769682	36178.906	246.9951	24.699507	0.011506924	0.00332749	0.00111
4400	460.7669225	276.4601535	37020.276	256.8393	25.683929	0.011693599	0.00338148	0.001128
4500	471.238898	282.7433388	37861.646	266.8414	26.684138	0.011879005	0.00343509	0.001146
4600	481.7108736	289.0265241	38703.016	277.0003	27.700029	0.01206318	0.00348835	0.001164
4700	492.1828491	295.3097094	39544.386	287.315	28.731498	0.012246157	0.00354126	0.001182
4800	502.6548246	301.5928947	40385.756	297.7844	29.778445	0.01242797	0.00359384	0.001199
4900	513.1268001	307.8760801	41227.126	308.4077	30.840772	0.012608649	0.00364608	0.001217
5000	523.5987756	314.1592654	42068.495	319.1839	31.918386	0.012788226	0.00369801	0.001234

ANNEX 4 – Corresponding RCE rotation rates for a range of flow rates of water in different sizes of Schedule 40 pipes

In order to use the following table, cross the row of the flow rate in the pipe with the column with the internal diameter of the Schedule 40 Type pipe. The cell at the intersection will give the corresponding RCE rotation rate (in RPM) which needs to be used to simulate the respective flow in a lab environment. The cells highlighted in **green** show the rotation rate values which are **not usable** with the Autolab RCE system.

Table 3 – Correlation between flow rates and RCE rotation rates for different sizes of Schedule 40 pipes. The fluid is water, with a smooth and straight flow. These quantities assume a 12 mm RCE cylindrical insert, rotated in water at 25 °C (density is 0.997 g cm^{-3}).

Flow rate in the Pipe			Schedule 40 Type	1 inch	2 inch	3 inch	4 inch	5 inch	6 inch	8 inch	10 inch	12 inch	14 inch	16 inch	18 inch	20 inch	24 inch
ft s^{-1}	cm s^{-1}	mi h^{-1}	Pipe ID (cm)	2.66	5.25	7.79	10.23	12.82	15.41	20.27	25.45	30.32	33.35	38.10	42.88	47.78	57.48
0.1	3.048	0.068		13	11	10	10	9	9	9	8	8	8	8	8	7	7
0.2	6.096	0.136		30	26	25	23	22	22	21	20	19	19	19	18	18	17
0.3	9.144	0.205		49	44	41	39	37	36	34	33	32	31	31	30	30	29
0.4	12.19	0.273		71	63	58	56	53	52	49	47	46	45	44	43	42	41
0.5	15.24	0.341		94	83	77	74	71	68	65	63	61	60	58	57	56	54
0.6	18.29	0.409		118	104	97	92	89	86	82	79	76	75	73	72	70	68
0.7	21.34	0.477		142	126	118	112	108	104	99	95	92	91	89	87	85	82
0.8	24.38	0.545		168	149	139	132	127	123	117	113	109	107	105	103	101	97
0.9	27.43	0.614		195	173	161	153	147	143	136	130	126	124	121	119	116	113
1	30.48	0.682		223	197	184	175	168	163	155	149	144	142	138	135	133	129
1.1	33.53	0.75		251	222	207	197	189	183	174	168	162	160	156	153	150	145
1.2	36.58	0.818		279	248	231	220	211	204	195	187	181	178	174	170	167	161
1.3	39.62	0.886		309	274	255	243	233	226	215	206	200	197	192	188	184	178
1.4	42.67	0.955		339	300	280	267	256	248	236	226	220	216	211	206	202	196
1.5	45.72	1.023		369	327	305	291	279	270	257	247	239	235	230	225	221	213
1.6	48.77	1.091		400	355	331	315	302	293	279	268	259	255	249	244	239	231
1.7	51.82	1.159		432	383	357	340	326	316	301	289	280	275	269	263	258	250
1.8	54.86	1.227		464	411	383	365	350	339	323	310	301	295	289	282	277	268
1.9	57.91	1.295		496	440	410	390	375	363	346	332	322	316	309	302	296	287
2	60.96	1.364		529	469	437	416	400	387	368	354	343	337	329	322	316	306
2.1	64.01	1.432		563	498	464	442	425	411	392	376	364	358	350	343	336	325

Flow rate in the Pipe			Schedule 40 Type	1 inch	2 inch	3 inch	4 inch	5 inch	6 inch	8 inch	10 inch	12 inch	14 inch	16 inch	18 inch	20 inch	24 inch
ft s^{-1}	cm s^{-1}	mi h^{-1}	Pipe ID (cm)	2.66	5.25	7.79	10.23	12.82	15.41	20.27	25.45	30.32	33.35	38.10	42.88	47.78	57.48
2.2	67.06	1.5		596	528	492	469	450	436	415	398	386	380	371	363	356	345
2.3	70.1	1.568		630	558	520	496	476	461	439	421	408	401	392	384	376	364
2.4	73.15	1.636		665	589	549	523	502	486	463	444	431	423	413	405	397	384
2.5	76.2	1.705		700	620	578	550	528	511	487	468	453	445	435	426	418	404
2.6	79.25	1.773		735	651	607	578	555	537	511	491	476	468	457	447	439	425
2.7	82.3	1.841		770	682	636	606	582	563	536	515	499	490	479	469	460	445
2.8	85.34	1.909		806	714	665	634	609	589	561	539	522	513	501	491	481	466
2.9	88.39	1.977		842	746	695	662	636	616	586	563	545	536	524	513	503	487
3	91.44	2.045		879	778	725	691	664	642	612	587	569	559	546	535	525	508
3.1	94.49	2.114		915	811	756	720	691	669	637	612	593	583	569	557	547	529
3.2	97.54	2.182		952	844	786	749	719	696	663	637	617	607	592	580	569	550
3.3	100.6	2.25		990	877	817	778	748	723	689	661	641	630	615	603	591	572
3.4	103.6	2.318		1027	910	848	808	776	751	715	687	665	654	639	626	614	594
3.5	106.7	2.386		1065	944	880	838	805	779	741	712	690	678	662	649	636	616
3.6	109.7	2.455		1103	978	911	868	834	807	768	737	715	703	686	672	659	638
3.7	112.8	2.523		1142	1012	943	898	863	835	795	763	740	727	710	695	682	660
3.8	115.8	2.591		1181	1046	975	928	892	863	822	789	765	752	734	719	705	682
3.9	118.9	2.659		1220	1080	1007	959	921	891	849	815	790	777	758	743	728	705
4	121.9	2.727		1259	1115	1039	990	951	920	876	841	815	802	783	766	752	727
4.1	125	2.795		1298	1150	1072	1021	981	949	904	868	841	827	807	790	775	750
4.2	128	2.864		1338	1185	1105	1052	1011	978	931	894	867	852	832	815	799	773
4.3	131.1	2.932		1378	1221	1138	1084	1041	1007	959	921	893	877	857	839	823	796
4.4	134.1	3		1418	1256	1171	1115	1071	1037	987	948	919	903	882	863	847	819
4.5	137.2	3.068		1459	1292	1204	1147	1102	1066	1015	975	945	929	907	888	871	843
4.6	140.2	3.136		1499	1328	1238	1179	1132	1096	1043	1002	971	955	932	913	895	866
4.7	143.3	3.205		1540	1364	1271	1211	1163	1126	1072	1029	997	981	958	938	920	890
4.8	146.3	3.273		1581	1401	1305	1243	1194	1156	1100	1057	1024	1007	983	963	944	914
4.9	149.4	3.341		1622	1437	1339	1276	1225	1186	1129	1084	1051	1033	1009	988	969	937
5	152.4	3.409		1664	1474	1374	1308	1257	1216	1158	1112	1078	1060	1035	1013	994	961
5.1	155.4	3.477		1706	1511	1408	1341	1288	1247	1187	1140	1105	1086	1061	1038	1019	985

Flow rate in the Pipe			Schedule 40 Type	1 inch	2 inch	3 inch	4 inch	5 inch	6 inch	8 inch	10 inch	12 inch	14 inch	16 inch	18 inch	20 inch	24 inch
ft s^{-1}	cm s^{-1}	mi h^{-1}	Pipe ID (cm)	2.66	5.25	7.79	10.23	12.82	15.41	20.27	25.45	30.32	33.35	38.10	42.88	47.78	57.48
5.2	158.5	3.545		1747	1548	1443	1374	1320	1277	1216	1168	1132	1113	1087	1064	1044	1010
5.3	161.5	3.614		1790	1585	1477	1407	1352	1308	1246	1196	1159	1140	1113	1090	1069	1034
5.4	164.6	3.682		1832	1623	1512	1441	1384	1339	1275	1224	1187	1167	1139	1115	1094	1058
5.5	167.6	3.75		1874	1660	1547	1474	1416	1370	1305	1253	1214	1194	1166	1141	1119	1083
5.6	170.7	3.818		1917	1698	1583	1508	1448	1401	1334	1281	1242	1221	1192	1167	1145	1108
5.7	173.7	3.886		1960	1736	1618	1541	1480	1433	1364	1310	1269	1248	1219	1193	1170	1132
5.8	176.8	3.955		2003	1774	1654	1575	1513	1464	1394	1339	1297	1276	1246	1220	1196	1157
5.9	179.8	4.023		2046	1813	1689	1609	1546	1496	1424	1368	1325	1303	1272	1246	1222	1182
6	182.9	4.091		2090	1851	1725	1643	1578	1527	1454	1397	1354	1331	1299	1272	1248	1207
6.1	185.9	4.159		2133	1890	1761	1678	1611	1559	1485	1426	1382	1359	1327	1299	1274	1233
6.2	189	4.227		2177	1929	1797	1712	1644	1591	1515	1455	1410	1386	1354	1326	1300	1258
6.3	192	4.295		2221	1968	1834	1747	1678	1623	1546	1484	1439	1414	1381	1352	1326	1283
6.4	195.1	4.364		2265	2007	1870	1781	1711	1656	1577	1514	1467	1443	1409	1379	1353	1309
6.5	198.1	4.432		2310	2046	1907	1816	1745	1688	1608	1543	1496	1471	1436	1406	1379	1335
6.6	201.2	4.5		2354	2085	1944	1851	1778	1721	1638	1573	1525	1499	1464	1433	1406	1360
6.7	204.2	4.568		2399	2125	1980	1886	1812	1753	1670	1603	1554	1528	1492	1461	1433	1386
6.8	207.3	4.636		2444	2165	2017	1922	1846	1786	1701	1633	1583	1556	1520	1488	1459	1412
6.9	210.3	4.705		2489	2205	2055	1957	1880	1819	1732	1663	1612	1585	1548	1515	1486	1438
7	213.4	4.773		2534	2245	2092	1993	1914	1852	1764	1693	1641	1614	1576	1543	1513	1464
7.1	216.4	4.841		2579	2285	2129	2028	1948	1885	1795	1724	1671	1642	1604	1570	1540	1490
7.2	219.5	4.909		2625	2325	2167	2064	1982	1918	1827	1754	1700	1671	1632	1598	1567	1517
7.3	222.5	4.977		2670	2366	2205	2100	2017	1952	1859	1785	1730	1700	1660	1626	1595	1543
7.4	225.6	5.045		2716	2406	2242	2136	2052	1985	1890	1815	1759	1730	1689	1654	1622	1569
7.5	228.6	5.114		2762	2447	2280	2172	2086	2019	1922	1846	1789	1759	1718	1682	1649	1596
7.6	231.6	5.182		2808	2488	2318	2208	2121	2053	1954	1877	1819	1788	1746	1710	1677	1623
7.7	234.7	5.25		2854	2529	2357	2245	2156	2086	1987	1908	1849	1818	1775	1738	1705	1649
7.8	237.7	5.318		2901	2570	2395	2281	2191	2120	2019	1939	1879	1847	1804	1766	1732	1676
7.9	240.8	5.386		2947	2611	2433	2318	2226	2154	2051	1970	1909	1877	1833	1795	1760	1703
8	243.8	5.455		2994	2652	2472	2355	2262	2188	2084	2001	1939	1907	1862	1823	1788	1730
8.1	246.9	5.523		3041	2694	2511	2391	2297	2223	2117	2032	1970	1936	1891	1851	1816	1757
8.2	249.9	5.591		3088	2736	2549	2428	2332	2257	2149	2064	2000	1966	1920	1880	1844	1784

Flow rate in the Pipe			Schedule 40 Type	1 inch	2 inch	3 inch	4 inch	5 inch	6 inch	8 inch	10 inch	12 inch	14 inch	16 inch	18 inch	20 inch	24 inch
ft s^{-1}	cm s^{-1}	mi h^{-1}	Pipe ID (cm)	2.66	5.25	7.79	10.23	12.82	15.41	20.27	25.45	30.32	33.35	38.10	42.88	47.78	57.48
8.3	253	5.659		3135	2777	2588	2465	2368	2292	2182	2095	2031	1996	1949	1909	1872	1811
8.4	256	5.727		3182	2819	2627	2503	2404	2326	2215	2127	2061	2027	1979	1938	1901	1839
8.5	259.1	5.795		3230	2861	2666	2540	2440	2361	2248	2158	2092	2057	2008	1966	1929	1866
8.6	262.1	5.864		3277	2903	2706	2577	2476	2395	2281	2190	2123	2087	2038	1995	1957	1894
8.7	265.2	5.932		3325	2946	2745	2615	2512	2430	2314	2222	2154	2117	2068	2024	1986	1921
8.8	268.2	6		3373	2988	2785	2652	2548	2465	2348	2254	2185	2148	2097	2054	2014	1949
8.9	271.3	6.068		3421	3031	2824	2690	2584	2500	2381	2286	2216	2178	2127	2083	2043	1977
9	274.3	6.136		3469	3073	2864	2728	2620	2536	2414	2318	2247	2209	2157	2112	2072	2004
9.1	277.4	6.205		3517	3116	2904	2766	2657	2571	2448	2351	2278	2240	2187	2141	2100	2032
9.2	280.4	6.273		3566	3159	2944	2804	2693	2606	2482	2383	2310	2271	2217	2171	2129	2060
9.3	283.5	6.341		3614	3202	2984	2842	2730	2642	2515	2415	2341	2301	2247	2200	2158	2088
9.4	286.5	6.409		3663	3245	3024	2880	2767	2677	2549	2448	2372	2332	2278	2230	2187	2116
9.5	289.6	6.477		3711	3288	3064	2919	2803	2713	2583	2480	2404	2363	2308	2260	2217	2145
9.6	292.6	6.545		3760	3331	3105	2957	2840	2749	2617	2513	2436	2395	2338	2290	2246	2173
9.7	295.7	6.614		3809	3375	3145	2996	2877	2784	2651	2546	2467	2426	2369	2319	2275	2201
9.8	298.7	6.682		3859	3418	3186	3034	2915	2820	2686	2579	2499	2457	2399	2349	2304	2230
9.9	301.8	6.75		3908	3462	3226	3073	2952	2856	2720	2612	2531	2489	2430	2379	2334	2258
10	304.8	6.818		3957	3506	3267	3112	2989	2892	2754	2645	2563	2520	2461	2409	2363	2287
10.1	307.8	6.886		4007	3550	3308	3151	3027	2929	2789	2678	2595	2552	2492	2440	2393	2315
10.2	310.9	6.955		4056	3594	3349	3190	3064	2965	2823	2711	2627	2583	2522	2470	2423	2344
10.3	313.9	7.023		4106	3638	3390	3229	3102	3001	2858	2744	2660	2615	2553	2500	2452	2373
10.4	317	7.091		4156	3682	3431	3268	3139	3038	2893	2778	2692	2647	2584	2530	2482	2401
10.5	320	7.159		4206	3726	3473	3308	3177	3074	2928	2811	2724	2678	2616	2561	2512	2430
10.6	323.1	7.227		4256	3771	3514	3347	3215	3111	2962	2844	2757	2710	2647	2591	2542	2459
10.7	326.1	7.295		4306	3815	3555	3387	3253	3148	2997	2878	2789	2742	2678	2622	2572	2488
10.8	329.2	7.364		4357	3860	3597	3426	3291	3185	3032	2912	2822	2774	2709	2653	2602	2517
10.9	332.2	7.432		4407	3904	3639	3466	3329	3221	3068	2945	2855	2807	2741	2683	2632	2547
11	335.3	7.5		4458	3949	3680	3506	3367	3258	3103	2979	2888	2839	2772	2714	2662	2576
11.1	338.3	7.568		4509	3994	3722	3546	3406	3296	3138	3013	2920	2871	2804	2745	2693	2605
11.2	341.4	7.636		4559	4039	3764	3586	3444	3333	3173	3047	2953	2903	2835	2776	2723	2635
11.3	344.4	7.705		4610	4084	3806	3626	3482	3370	3209	3081	2986	2936	2867	2807	2753	2664

Flow rate in the Pipe			Schedule 40 Type	1 inch	2 inch	3 inch	4 inch	5 inch	6 inch	8 inch	10 inch	12 inch	14 inch	16 inch	18 inch	20 inch	24 inch
ft s^{-1}	cm s^{-1}	mi h^{-1}	Pipe ID (cm)	2.66	5.25	7.79	10.23	12.82	15.41	20.27	25.45	30.32	33.35	38.10	42.88	47.78	57.48
11.4	347.5	7.773		4661	4130	3848	3666	3521	3407	3244	3115	3019	2968	2899	2838	2784	2693
11.5	350.5	7.841		4713	4175	3891	3706	3560	3445	3280	3149	3053	3001	2931	2869	2814	2723
11.6	353.6	7.909		4764	4220	3933	3746	3598	3482	3316	3184	3086	3034	2962	2901	2845	2753
11.7	356.6	7.977		4815	4266	3975	3787	3637	3520	3352	3218	3119	3066	2994	2932	2876	2782
11.8	359.7	8.045		4867	4312	4018	3827	3676	3557	3387	3252	3152	3099	3026	2963	2907	2812
11.9	362.7	8.114		4918	4357	4061	3868	3715	3595	3423	3287	3186	3132	3058	2995	2937	2842
12	365.8	8.182		4970	4403	4103	3909	3754	3633	3459	3322	3219	3165	3091	3026	2968	2872
12.1	368.8	8.25		5022	4449	4146	3949	3793	3671	3495	3356	3253	3198	3123	3058	2999	2902
12.2	371.9	8.318		5074	4495	4189	3990	3833	3709	3532	3391	3287	3231	3155	3089	3030	2932
12.3	374.9	8.386		5126	4541	4232	4031	3872	3747	3568	3426	3320	3264	3188	3121	3061	2962
12.4	378	8.455		5178	4587	4275	4072	3911	3785	3604	3461	3354	3297	3220	3153	3092	2992
12.5	381	8.523		5230	4634	4318	4113	3951	3823	3640	3495	3388	3331	3252	3185	3124	3022
12.6	384	8.591		5283	4680	4361	4154	3990	3861	3677	3530	3422	3364	3285	3216	3155	3052
12.7	387.1	8.659		5335	4726	4405	4196	4030	3900	3713	3565	3456	3397	3318	3248	3186	3083
12.8	390.1	8.727		5388	4773	4448	4237	4070	3938	3750	3601	3490	3431	3350	3280	3218	3113
12.9	393.2	8.795		5440	4820	4492	4278	4109	3977	3787	3636	3524	3464	3383	3312	3249	3144
13	396.2	8.864		5493	4866	4535	4320	4149	4015	3823	3671	3558	3498	3416	3345	3281	3174
13.1	399.3	8.932		5546	4913	4579	4361	4189	4054	3860	3706	3592	3532	3449	3377	3312	3205
13.2	402.3	9		5599	4960	4622	4403	4229	4093	3897	3742	3627	3565	3482	3409	3344	3235
13.3	405.4	9.068		5652	5007	4666	4445	4269	4131	3934	3777	3661	3599	3515	3441	3375	3266
13.4	408.4	9.136		5705	5054	4710	4487	4309	4170	3971	3813	3695	3633	3548	3474	3407	3297
13.5	411.5	9.205		5758	5101	4754	4529	4350	4209	4008	3848	3730	3667	3581	3506	3439	3327
13.6	414.5	9.273		5812	5149	4798	4571	4390	4248	4045	3884	3765	3701	3614	3539	3471	3358
13.7	417.6	9.341		5865	5196	4842	4613	4430	4287	4082	3920	3799	3735	3647	3571	3503	3389
13.8	420.6	9.409		5919	5244	4887	4655	4471	4326	4120	3956	3834	3769	3681	3604	3535	3420
13.9	423.7	9.477		5973	5291	4931	4697	4511	4366	4157	3991	3869	3803	3714	3636	3567	3451
14	426.7	9.545		6026	5339	4975	4739	4552	4405	4194	4027	3903	3838	3747	3669	3599	3482
14.1	429.8	9.614		6080	5386	5020	4782	4593	4444	4232	4063	3938	3872	3781	3702	3631	3513
14.2	432.8	9.682		6134	5434	5064	4824	4633	4484	4269	4099	3973	3906	3814	3735	3663	3544
14.3	435.9	9.75		6188	5482	5109	4866	4674	4523	4307	4136	4008	3941	3848	3768	3696	3576
14.4	438.9	9.818		6242	5530	5154	4909	4715	4563	4345	4172	4043	3975	3882	3801	3728	3607

Flow rate in the Pipe			Schedule 40 Type	1 inch	2 inch	3 inch	4 inch	5 inch	6 inch	8 inch	10 inch	12 inch	14 inch	16 inch	18 inch	20 inch	24 inch
ft s^{-1}	cm s^{-1}	mi h^{-1}	Pipe ID (cm)	2.66	5.25	7.79	10.23	12.82	15.41	20.27	25.45	30.32	33.35	38.10	42.88	47.78	57.48
14.5	442	9.886		6297	5578	5198	4952	4756	4602	4383	4208	4078	4010	3915	3834	3760	3638
14.6	445	9.955		6351	5626	5243	4994	4797	4642	4420	4244	4114	4044	3949	3867	3793	3670
14.7	448.1	10.02		6405	5674	5288	5037	4838	4682	4458	4281	4149	4079	3983	3900	3825	3701
14.8	451.1	10.09		6460	5723	5333	5080	4879	4722	4496	4317	4184	4114	4017	3933	3858	3733
14.9	454.2	10.16		6514	5771	5378	5123	4921	4762	4534	4354	4220	4148	4051	3966	3890	3764
15	457.2	10.23		6569	5820	5423	5166	4962	4802	4572	4390	4255	4183	4085	4000	3923	3796
15.1	460.2	10.3		6624	5868	5469	5209	5003	4842	4610	4427	4290	4218	4119	4033	3956	3827
15.2	463.3	10.36		6679	5917	5514	5252	5045	4882	4649	4463	4326	4253	4153	4066	3989	3859
15.3	466.3	10.43		6734	5965	5559	5296	5086	4922	4687	4500	4362	4288	4187	4100	4021	3891
15.4	469.4	10.5		6789	6014	5605	5339	5128	4962	4725	4537	4397	4323	4222	4133	4054	3923
15.5	472.4	10.57		6844	6063	5650	5382	5170	5002	4764	4574	4433	4358	4256	4167	4087	3955
15.6	475.5	10.64		6899	6112	5696	5426	5211	5043	4802	4611	4469	4393	4290	4201	4120	3986
15.7	478.5	10.7		6955	6161	5742	5469	5253	5083	4840	4648	4505	4429	4325	4234	4153	4018
15.8	481.6	10.77		7010	6210	5787	5513	5295	5124	4879	4685	4541	4464	4359	4268	4186	4050
15.9	484.6	10.84		7065	6259	5833	5556	5337	5164	4918	4722	4576	4499	4394	4302	4220	4083
16	487.7	10.91		7121	6309	5879	5600	5379	5205	4956	4759	4612	4535	4428	4336	4253	4115
16.1	490.7	10.98		7177	6358	5925	5644	5421	5246	4995	4796	4649	4570	4463	4370	4286	4147
16.2	493.8	11.05		7232	6407	5971	5688	5463	5286	5034	4833	4685	4606	4497	4404	4319	4179
16.3	496.8	11.11		7288	6457	6017	5732	5505	5327	5073	4871	4721	4641	4532	4438	4353	4211
16.4	499.9	11.18		7344	6506	6063	5776	5548	5368	5112	4908	4757	4677	4567	4472	4386	4244
16.5	502.9	11.25		7400	6556	6110	5820	5590	5409	5151	4946	4793	4713	4602	4506	4420	4276
16.6	506	11.32		7456	6606	6156	5864	5632	5450	5190	4983	4830	4748	4637	4540	4453	4308
16.7	509	11.39		7513	6655	6202	5908	5675	5491	5229	5021	4866	4784	4672	4574	4487	4341
16.8	512.1	11.45		7569	6705	6249	5952	5717	5532	5268	5058	4903	4820	4707	4608	4520	4373
16.9	515.1	11.52		7625	6755	6295	5997	5760	5574	5307	5096	4939	4856	4742	4643	4554	4406
17	518.2	11.59		7682	6805	6342	6041	5802	5615	5347	5134	4976	4892	4777	4677	4588	4439
17.1	521.2	11.66		7738	6855	6389	6085	5845	5656	5386	5171	5012	4928	4812	4712	4621	4471
17.2	524.3	11.73		7795	6905	6435	6130	5888	5697	5425	5209	5049	4964	4847	4746	4655	4504
17.3	527.3	11.8		7851	6956	6482	6175	5931	5739	5465	5247	5086	5000	4882	4780	4689	4537
17.4	530.4	11.86		7908	7006	6529	6219	5974	5780	5504	5285	5122	5036	4918	4815	4723	4569
17.5	533.4	11.93		7965	7056	6576	6264	6016	5822	5544	5323	5159	5072	4953	4850	4757	4602

Flow rate in the Pipe			Schedule 40 Type	1 inch	2 inch	3 inch	4 inch	5 inch	6 inch	8 inch	10 inch	12 inch	14 inch	16 inch	18 inch	20 inch	24 inch
ft s^{-1}	cm s^{-1}	mi h^{-1}	Pipe ID (cm)	2.66	5.25	7.79	10.23	12.82	15.41	20.27	25.45	30.32	33.35	38.10	42.88	47.78	57.48
17.6	536.4	12		8022	7107	6623	6309	6059	5864	5583	5361	5196	5108	4988	4884	4791	4635
17.7	539.5	12.07		8079	7157	6670	6353	6103	5905	5623	5399	5233	5145	5024	4919	4825	4668
17.8	542.5	12.14		8136	7208	6717	6398	6146	5947	5663	5437	5270	5181	5059	4954	4859	4701
17.9	545.6	12.2		8193	7258	6764	6443	6189	5989	5703	5476	5307	5218	5095	4989	4893	4734
18	548.6	12.27		8251	7309	6812	6488	6232	6031	5743	5514	5344	5254	5131	5023	4927	4767
18.1	551.7	12.34		8308	7360	6859	6533	6275	6073	5782	5552	5381	5290	5166	5058	4962	4800
18.2	554.7	12.41		8365	7411	6906	6579	6319	6115	5822	5591	5418	5327	5202	5093	4996	4834
18.3	557.8	12.48		8423	7462	6954	6624	6362	6157	5862	5629	5456	5364	5238	5128	5030	4867
18.4	560.8	12.55		8480	7513	7001	6669	6406	6199	5902	5667	5493	5400	5273	5163	5065	4900
18.5	563.9	12.61		8538	7564	7049	6714	6449	6241	5943	5706	5530	5437	5309	5199	5099	4933
18.6	566.9	12.68		8596	7615	7097	6760	6493	6283	5983	5745	5568	5474	5345	5234	5133	4967
18.7	570	12.75		8654	7666	7144	6805	6536	6325	6023	5783	5605	5511	5381	5269	5168	5000
18.8	573	12.82		8711	7718	7192	6851	6580	6368	6063	5822	5643	5547	5417	5304	5203	5034
18.9	576.1	12.89		8769	7769	7240	6896	6624	6410	6104	5861	5680	5584	5453	5339	5237	5067
19	579.1	12.95		8827	7820	7288	6942	6668	6452	6144	5899	5718	5621	5489	5375	5272	5101
19.1	582.2	13.02		8886	7872	7336	6988	6712	6495	6185	5938	5755	5658	5525	5410	5307	5134
19.2	585.2	13.09		8944	7923	7384	7034	6756	6537	6225	5977	5793	5695	5562	5446	5341	5168
19.3	588.3	13.16		9002	7975	7432	7079	6800	6580	6266	6016	5831	5733	5598	5481	5376	5201
19.4	591.3	13.23		9060	8027	7480	7125	6844	6623	6306	6055	5869	5770	5634	5517	5411	5235
19.5	594.4	13.3		9119	8078	7528	7171	6888	6665	6347	6094	5906	5807	5670	5552	5446	5269
19.6	597.4	13.36		9177	8130	7577	7217	6932	6708	6388	6133	5944	5844	5707	5588	5481	5303
19.7	600.5	13.43		9236	8182	7625	7263	6976	6751	6428	6172	5982	5881	5743	5623	5516	5337
19.8	603.5	13.5		9294	8234	7673	7309	7021	6794	6469	6211	6020	5919	5780	5659	5551	5370
19.9	606.6	13.57		9353	8286	7722	7355	7065	6837	6510	6251	6058	5956	5816	5695	5586	5404
20	609.6	13.64		9412	8338	7770	7402	7109	6880	6551	6290	6096	5994	5853	5731	5621	5438